

## Article

# The influence of nicotine on trophoblast-derived exosomes in a mouse model of pathogenic preeclampsia

Ayane Kubo <sup>1</sup>, Keiichi Matsubara <sup>2\*</sup>, Yuko Matsubara <sup>1</sup>, Hiroto Nakaoka <sup>3</sup>, and Takashi Sugiyama <sup>1</sup>

<sup>1</sup> Department of Obstetrics and Gynecology, Ehime University School of Medicine, Shitsukawa, Toon, Ehime 791-0295, Japan; h401025x@mails.cc.ehime-u.ac.jp (A.K.); takeyu@m.ehime-u.ac.jp (Y.M.); sugiyama@m.ehime-u.ac.jp (T.S.)

<sup>2</sup> Department of Regional Pediatrics and Perinatology, Ehime University Graduate School of Medicine, Shitsukawa, Toon, Ehime 791-0295, Japan; keiichi@m.ehime-u.ac.jp

<sup>3</sup> Advanced Research Support Center, Ehime University Graduate School of Medicine, Shitsukawa, Toon, Ehime 791-0295, Japan; hnakaoka@m.ehime-u.ac.jp

\* Correspondence: keiichi@m.ehime-u.ac.jp; Tel.: +81-89-960-5379

**Abstract:** Preeclampsia (PE) is a serious complication of pregnancy with a pathogenesis that is not fully understood, though it involves the impaired invasion of extravillous trophoblasts (EVTs) into the decidual layer during implantation. Recently, others have found that diverse cell types, including EVT, produce exosomes filled with molecular cargo (mainly proteins and RNAs) that can be transported to other cells and organs both locally and long-range. The cargo delivered by exosomes can signal to and modify the receiving cells and their environment, and EVT-derived exosomes may influence the pathogenesis of PE. Because the risk of PE is actually decreased by cigarette smoking, we considered the possibility that nicotine, a critical component of tobacco smoke, might protect against PE by modifying the content of exosomes from EVTs. In this study, we applied nicotine stimulation to cultured EVTs and subjected their secreted exosomes to proteomic analysis. We identified many proteins whose abundance in exosomes was modified by nicotine treatment of the donor EVTs, and we used bioinformatic annotation and network analysis to select five key hub proteins with potential roles in the pathogenesis or prevention of PE.

**Keywords:** preeclampsia; exosomes; nicotine; proteomics; bioinformatics

## 1. Introduction

Preeclampsia (PE) is a serious, life-threatening disease that afflicts hypertensive pregnant women with symptoms that can include proteinuria, headaches, fetal growth restriction (FGR), liver and kidney dysfunction, seizures, and abnormal blood tests for coagulation and fetal factors. The development of PE often improves following delivery and may involve placental-derived factors, and a two-stage theory has been proposed to explain the pathogenesis [5, 6] (Fig. 1). In the first stage, extravillous trophoblasts (EVTs), which invade the uterine endometrium and myometrium in the first trimester of normal pregnancy, become functionally impaired, leading to disturbed remodeling of the spiral artery and poor placentation with uteroplacental ischemic defects. In the second stage, this dysfunctional placenta releases humoral factors into the maternal systemic circulation that lead to multi-organ damage and the hallmark symptoms of the disease. These factors, which include proinflammatory cytokines (e.g., tumor necrosis factor- $\alpha$  (TNF $\alpha$ ), and interferon- $\gamma$  (IFN- $\gamma$ )) and vasoactive substances (e.g., endothelin-1 (ET-1), thromboxane A<sub>2</sub>, and angiotensin II), can increase vasoconstriction, vascular permeability, and coagulopathy [1-4].

The mechanism by which EVTs influence the uterine tissue and distant organs is thought to involve exosomes, which are secreted extracellular vesicles loaded with molecular cargo (e.g., DNA, RNA, proteins), that travel to and communicate with recipient cells. These exosomes carry signals to create a local environment suitable for EVT

invasion, proliferation, and remodeling of the spiral artery, and these vesicles are also distributed more broadly to distant maternal organs in a strategy akin to that of cancer cell proliferation and invasion [7]. We are interested in the possibility that PE is initiated and maintained by the abnormal secretion and composition of EVT exosomes and therefore sought to examine exosome cargo for clues to the mechanism of influence on PE. To develop an experimental system in which the relationship between exosomes and PE pathogenesis can be manipulated, we took advantage of the observation that PE risk is reduced by tobacco smoking even though it increases other pregnancy risks (e.g., fetal growth restriction and placental abruption) [8, 9]. Because nicotine is a critical bioactive component of tobacco smoke that accumulates quickly in and affects many organs [10] [11, 12], we focused here on the possibility that nicotine acts on EVTs to modify exosome secretion and cargo composition in the context of PE pathogenesis.

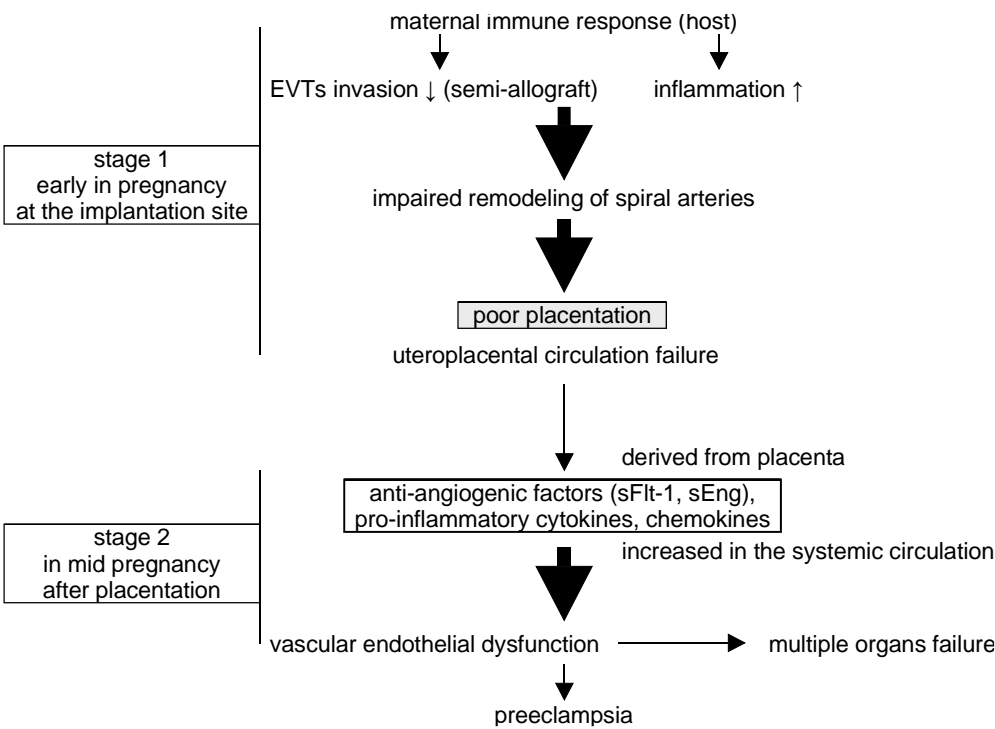


**Figure 1.** The two-stage theory of the pathogenesis of preeclampsia (PE). In stage one, abnormal placentation results from impaired EVT invasion and reduced immune tolerance for the fertilized egg. In stage two, the abnormal placenta produces anti-angiogenic factors and pro-inflammatory cytokines, resulting in multi-organ vascular dysfunction and the development of PE.

2. Results

This section may be divided by subheadings. It should provide a concise and precise description of the experimental results, their interpretation, as well as the experimental conclusions that can be drawn.

### 2.1. Physiologic effects of nicotine in a PE mouse model

The systolic BP of CD40L control mice gradually increased during pregnancy and remained elevated ( $120 \pm 6$  mmHg,  $n = 4$ ) through E17.5, while nicotine-treated mice had significantly lower systolic BP ( $107 \pm 4$  mmHg,  $n = 5$ ,  $p < .05$ ) at E17.5 (Fig. 2A).

Birth weights of pups were lower in the CD40L control group ( $1.31 \pm 0.41$  g,  $n = 9$ ) than the nicotine-treated group ( $1.46 \pm 0.35$  g,  $n = 7$ ), and placental weight was slightly lower in the control group ( $0.23 \pm 0.03$  g,  $n = 9$ ) compared with nicotine-treated mice ( $0.26 \pm 0.03$  g,  $n = 5$ ), though these results did not reach statistical significance (Fig. 2B). The urinary albumin/creatinine ratio was lower in nicotine-treated mice ( $0.08 \pm 0.04$  g,  $n = 5$ ) than control mice ( $0.35 \pm 0.11$  g,  $n = 4$ ) (Fig. 2C).

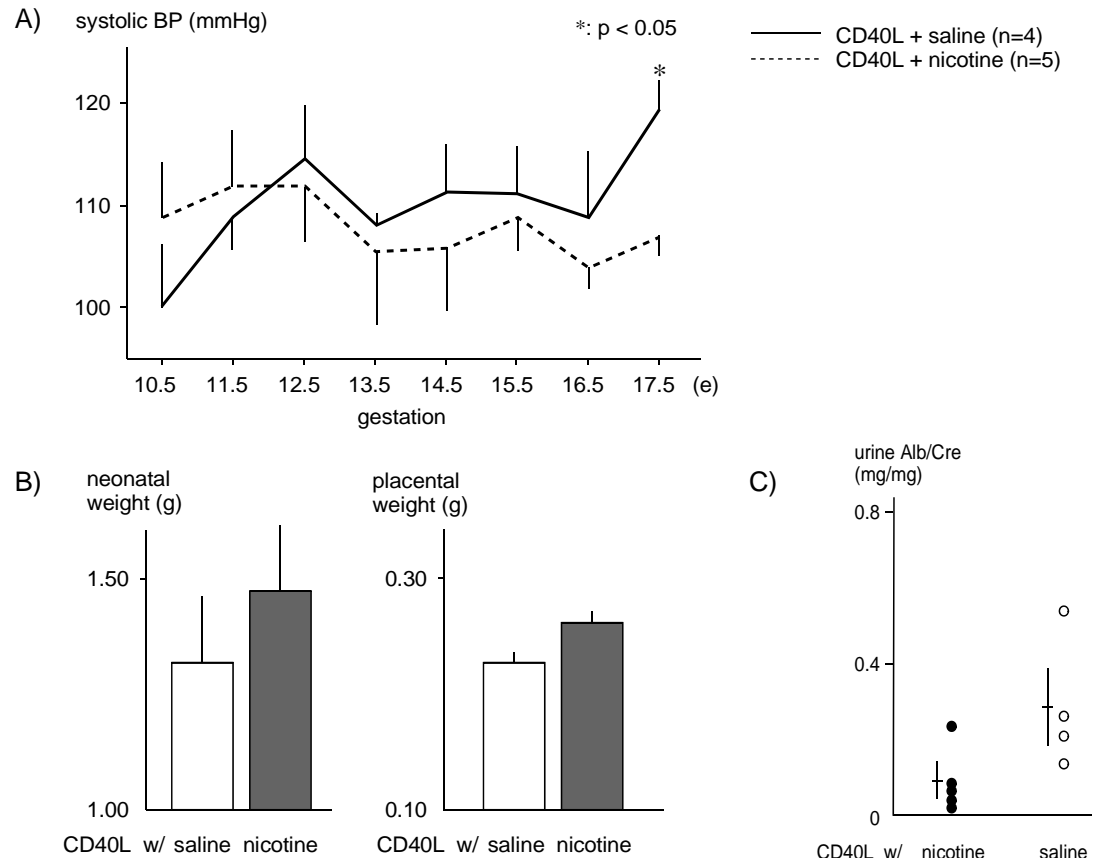


**Figure 2.** Physiologic effects of nicotine administration in PE model mice (A) Maternal systolic blood pressure during gestation. (B) Neonatal weight and placental weight of pups born from PE model mice. (C) Urinary albumin/creatinine ratio. \* $p < .05$ .

### 2.2. Proteomic analysis and bioinformatic characterization

Our proteomics analysis identified and qualified 2,477 proteins that we classified and annotated by several bioinformatics approaches. Using GO analysis, the proteins were organized by cellular component (Fig. 3A), biological process (Fig. 3B), and molecular function (Fig. 3C). Using PCA classification, we found clustering with high variance (Fig. 4) between the nicotine-treated and control groups. The nicotine group (pink) strongly expressed the characteristics of PC1 (36%), while the control group (orange) expressed the characteristics of PC2 (21%). The two groups were clearly separated, indicating that the protein composition of cultured EVT exosomes is strongly affected by nicotine. Using a volcano plot (Fig. 5), we identified 139 proteins (Table 1) that showed statistically significant and large-magnitude differences between the nicotine-treated and control groups (Fig. 5).

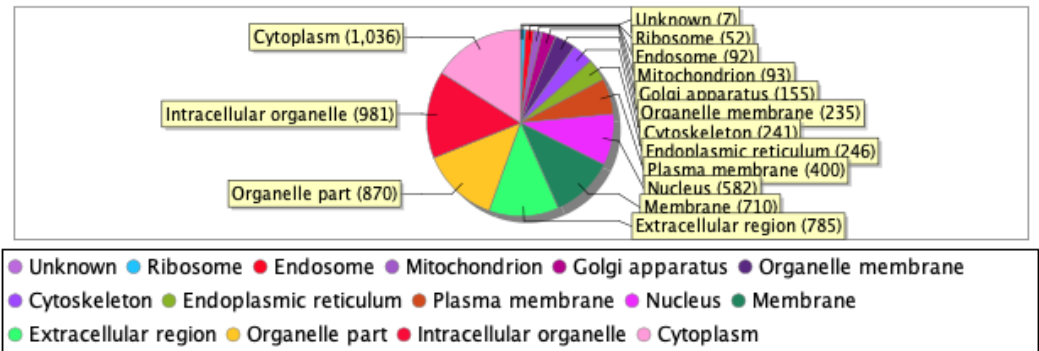


**Figure 3A.** Classification of EVT-derived exosome proteins organized by cellular component.

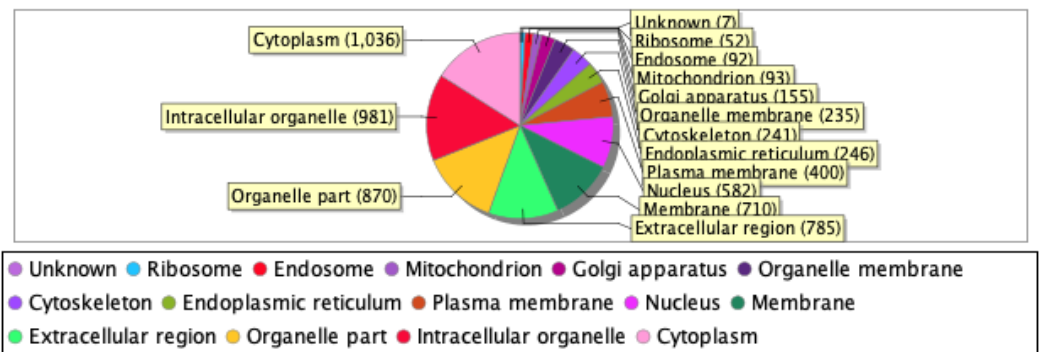


**Figure 3B.** Classification of EVT-derived exosome proteins organized by biological process.

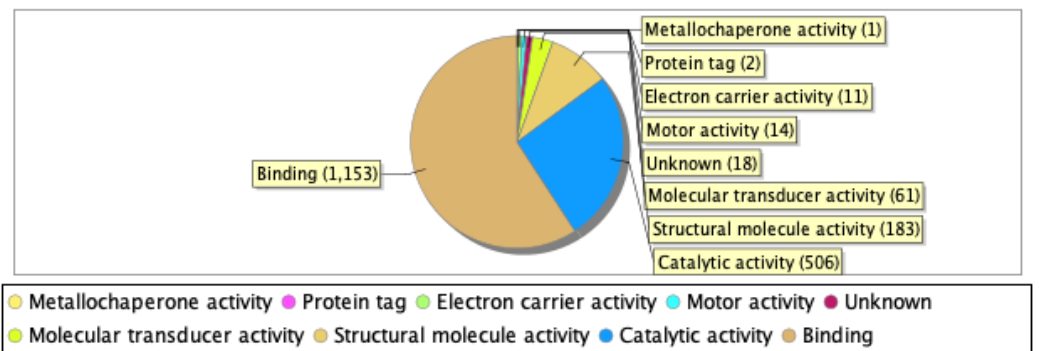


**Figure 3C.** Classification of EVT-derived exosome proteins organized by molecular function.

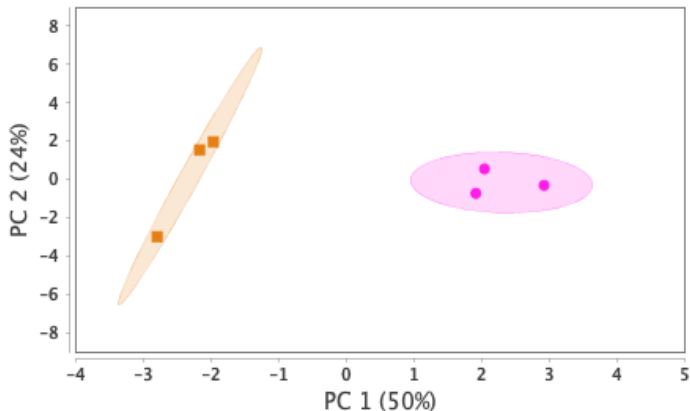


**Figure 4.** PCA score distribution of EVT-derived exosome proteins.

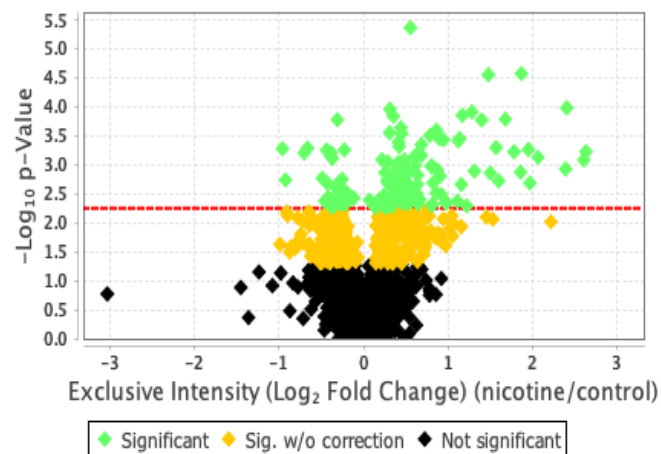


**Figure 5.** Classification of EVT-derived exosome proteins by p-value and differential abundance.

**Table 1.** Top ten proteins ranked by the magnitude of change (up- or down-regulated) and statistical significance (p-value) of differential abundance in control and nicotine-treated EVT-derived exosomes.

#### Upregulated

Accession number	Protein name	log2FC	p value
Q9UGI8	Testin	2.67	p < .05
Q02818	Nucleobindin-1	2.63	p < .001
P13591	Neural cell adhesion molecule 1	2.60	p < .001
P02788	Lactotransferrin	2.40	p < .0005
P28827	Receptor-type tyrosine-protein phosphatase mu	2.39	p < .005
P05114	Non-histone chromosomal protein HMG-14	2.31	p < .01
P24592	Insulin-like growth factor-binding protein 6	2.23	p < .05
P55285	Cadherin-6	2.21	p < .01
Q05682	Caldesmon	2.06	p < .001
O00533	Neural cell adhesion molecule L1-like protein	2.00	p < .005

#### Downregulated

Accession number	Protein name	log2FC	p value
Q6GTS8	N-fatty-acyl-amino acid synthase/hydrolase	-2.08	p < .0005
Q7Z7L7	Protein zer-1 homolog	-2.00	p < .05
Q14139	Serine/threonine-protein phosphatase 6 catalytic subunit	-1.78	p < .0005
Q14997	Proteasome activator complex subunit 4	-1.66	p < .05
Q03001	Dystonin	-1.51	p < .05
O60341	Lysine-specific histone demethylase 1A	-1.42	p < .0001
P68871	Hemoglobin subunit beta	-1.35	p < .05
P40306	Proteasome subunit beta type-10	-1.34	p < .05

Q9ULHO	Kinase D-interacting substrate of 220 kDa	-1.26	p < .001
Q13033	Striatin-3	-1.15	p < .005

### 2.3. Protein network analysis

The String database was used to analyze protein-protein interactions, and a network consisting of 42 nodes and 60 edges was found (Fig. 6). The proteins extracted by String analysis were further analyzed using Cytoscape Network Analyzer to search for nodes that serve as central network hubs (Fig. 7). In this analysis, we identified eight proteins with a high Degree that indicates network hub centrality, and further narrowed this list to five proteins: apolipoprotein A1 (APOA1); ceruloplasmin; kininogen 1; lumican; and KH domain-containing, RNA-binding, signal transduction-associated protein 1 (KHDRBS1). These proteins have the potential to influence PE pathogenesis based on their annotated biological properties and their differential abundance in nicotine-treated EVT exosomes.

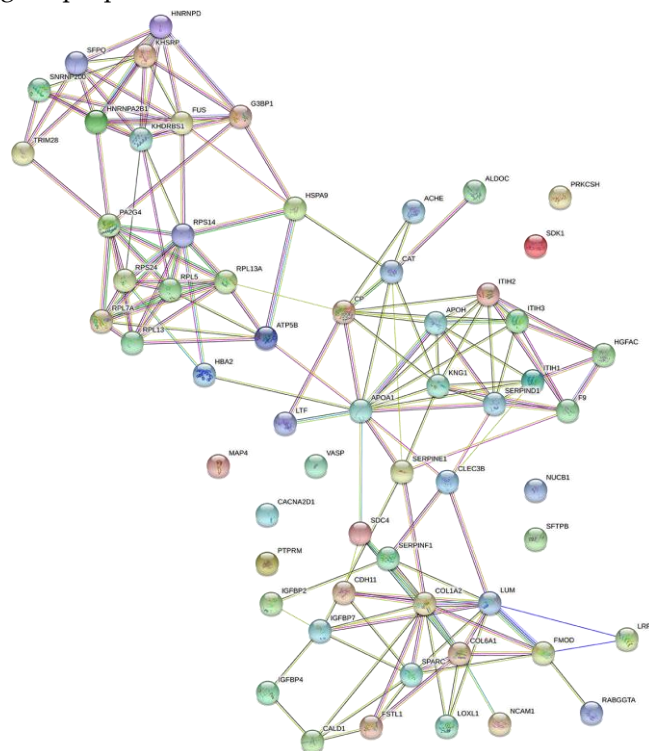


**Figure 6.** Protein-protein interaction network analysis of EVT-derived exosome proteins.



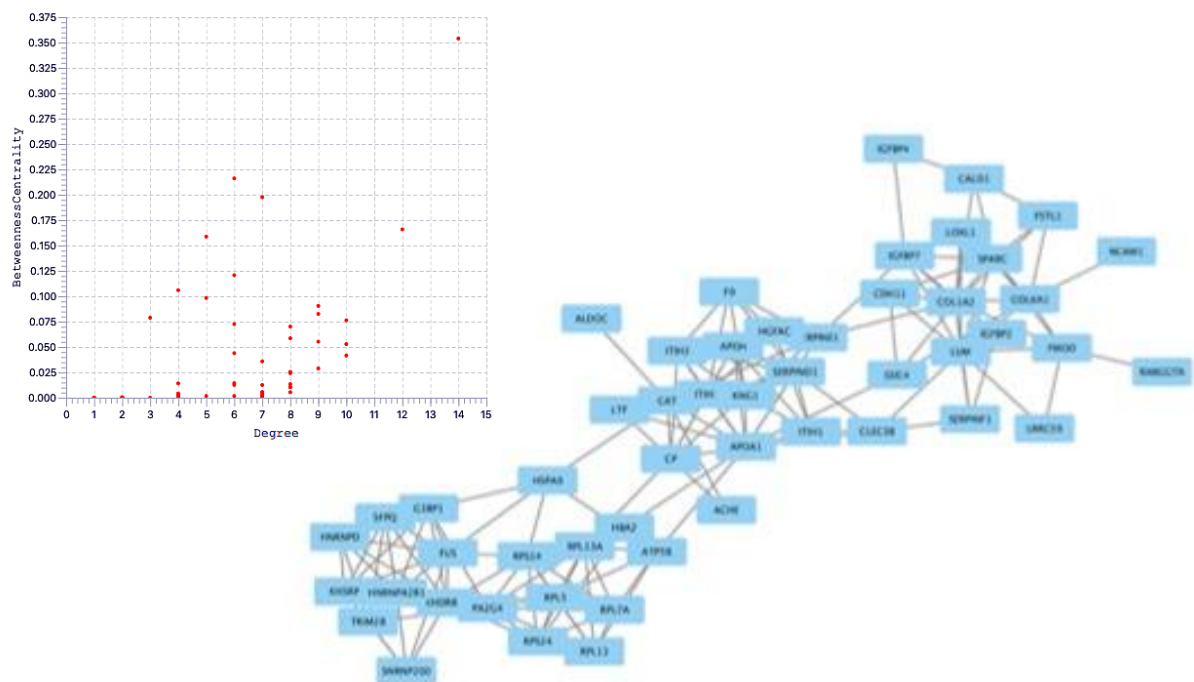


**Figure 7.** Top: Correlation between degree and betweenness centrality in EVT-derived exosome proteins, Bottom: Extracted key proteins.

### 3. Discussion

Nicotine is a critical component of tobacco smoke and a signaling molecule with diverse roles in the central nervous system and vasculature. Nicotine can either stimulate or inhibit ganglia (depending on dose) [14] and binds with nicotinic acetylcholine receptors (nAChRs) [14, 15] on several cell types to induce either vasoconstriction (when binding receptors on vascular endothelial cells) or vasodilation (when binding receptors on vascular smooth muscle cells). In the vascular endothelium, nicotine inhibits the release of the vasoconstrictor ET-1 [16] and inhibits the release of the vasodilators nitric oxide (NO) and prostacyclin [17] [18]. In vascular smooth muscle cells, nicotine promotes vasoconstriction by amplifying the response to norepinephrine and by upregulating the expression of ET-1 receptors (ETA and/or ETB) [19]. Thus, nicotine might promote the pathogenesis of PE by acting on vasoconstriction, but nicotine also exerts neuroprotective effects via nAChRs [11] and can suppress the onset of PE in pregnant women [9].

Exosomes can promote cancer growth and metastasis by forming a microenvironment around cancer cells that is protective against genotoxic stress-induced cell death [20]. The cargo within these exosomes can create conditions favorable for tumor growth when acting on local tissues and promotes metastasis when transported by exosomes to distant organs. During pregnancy, EVTs take on a role analogous to that of a cancer cell by secreting exosomes that create a microenvironment protective against autoimmunity and inflammation and supportive of EVT proliferation at the implantation site, placenta, and in distant organs.

In this study, we identified and quantified 2,477 proteins from the exosomes of nicotine-treated EVTs. Exosomes in the placenta are mainly released from the trophoblast and are thought to influence endometrial function and create a suitable placental environment [20]. Many of these proteins have predicted cytoplasmic localization, and 1,118 proteins are involved in cellular processes (e.g., transcription, DNA replication, and DNA repair) that are common in the trophoblast cell lineage. The majority of the proteins are predicted to have a molecular binding function. Su et al. reported that proteins in the trophoblast-derived exosome are enriched in immune and endocrine functions [21], though the five

hub proteins that we identified as differentially abundant in nicotine-treated EVT exosomes have functions related to cell proliferation and invasion.

APOA1 is the major protein component of high-density lipoprotein (HDL), which is synthesized in the liver and small intestine. It is associated with cholesterol transport, lipid-cholesterol binding, lecithin cholesterol acyltransferase (LCAT) activation. LCAT may activate HDL remodeling protein [22]. In PE, the proinflammatory cytokine TNF $\alpha$  is elevated from early pregnancy and may be involved in the pathogenesis of the disease. APOA1 suppresses this effect and might prevent TNF $\alpha$  from damaging EVTs [23].

KHDRBS1 is a protein implicated in selective splicing, cell cycle regulation, RNA 3'-end formation, and tumorigenesis. KHDRBS1 regulates the nuclear-to-cytoplasmic signaling that activates NF- $\kappa$ B proteins in response to DNA damage. A deficiency in KHDRBS1 reduces this signaling and dampens NF- $\kappa$ B-mediated anti-apoptotic gene transcription, thus promoting cell death [24]. Nicotine can increase KHDRBS1 production by EVTs, suggesting that it inhibits cell death through inhibiting apoptosis. In addition, its predicted function in promoting cell proliferation and invasion suggests that it may alter the proliferation of trophoblast ectoderm cells and promote placentation in PE [23].

Alpha-2-thiol proteinase inhibitor is the precursor protein for high molecular weight kininogen, low molecular weight kininogen, and bradykinin. These factors are essential for blood coagulation and the construction of the kallikrein-kinin system. Bradykinin stimulates vascular endothelial cells to produce NO, which relaxes blood vessels and lowers blood pressure. Furthermore, bradykinin may influence placentation and obstruct the pathogenesis of PE by promoting the proliferation and invasion of trophoblasts [25, 26].

Lumican is an extracellular matrix protein associated with signal transduction in cancer cells and can have either pro- or anti-tumorigenic effects in different cancer types [27]. Lumican is involved in cellular processes associated with tumorigenesis, including epithelial-to-mesenchymal transition, cellular proliferation, migration, invasion, and adhesion [28].

Ceruloplasmin is the major copper transport protein in the blood, influences iron metabolism, and may scavenge reactive oxygen species, though much is still unknown about the exact function of this protein [29]. Ceruloplasmin inhibits cell proliferation and invasion of nasopharyngeal carcinoma and may inhibit EVT proliferation and invasion in placentation and thus promote the pathogenesis of PE [30]. Ceruloplasmin produced by IFN- $\gamma$ -stimulated monocytes promotes the ferroxidase activity that converts ferrous iron (Fe $^{2+}$ ) to ferric iron (Fe $^{3+}$ ). This activity inhibits the Fenton reaction between ferric iron and hydrogen peroxide responsible for harmful hydroxyl radicals.

The pathogenesis of PE entails aberrant placentation, and healthy placentation requires the successful remodeling of the spiral artery, which requires appropriate proliferation and invasion of EVTs. Nicotine can stimulate the migration and invasion of the esophageal squamous carcinoma cell line [32], suggesting that nicotine may also promote these processes in EVTs. Impaired remodeling of the spiral artery can result from acute or chronic inflammation early in pregnancy, and this inflammation can be driven by cytokines and reactive oxygen species. Nicotine reduces proinflammatory cytokine release from the placenta in LPS-induced PE model mice [34, 35]. The pathogenesis of PE may be promoted by increased placental growth factor production in EVTs [37] and placenta-derived exosomes might be involved in the maintenance of normal pregnancy through maternal-fetal tolerance [38].

Though it is generally accepted that smoking may suppress the onset of PE [9, 33], this benefit is only observed in Western populations but not in Asian populations [36]. This suggests that PE risk is also influenced by genetic predispositions and that tobacco smoke and nicotine may have complex and contradictory influences on the pathogenesis of PE. For example, although nicotine can promote the migration and invasion of some cell types, it can also inhibit EVT invasion by downregulating CXCL12 expression via nAChR [31].

In this study, we chose five hub proteins from nicotine-stimulated EVT-derived exosomes that may influence the pathogenesis of PE. APOA1 can obstruct the activity of



TNF $\alpha$ , which is increased in the serum of PE patients during early pregnancy [39]. Ceruloplasmin can suppress the elevated ROS production of the PE placenta and may influence vascular endothelial damage and trophoblast damage in the placenta [3]. Kininogen can lower blood pressure via vasodilation, and KHDRBS1 may stimulate placentation by inhibiting the secretion of proinflammatory cytokines and promoting cellular proliferation and invasion. Lumican may promote the poor placentation associated with PE by inhibiting cellular proliferation.

This study has a limitation. We evaluated the effects of nicotine and not smoking itself. Therefore, not all effects of smoking could be evaluated.

#### 4. Materials and Methods

##### 4.1. *Animal experiments with a PE mouse model*

We examined the effects of nicotine administration on PE-relevant physiological parameters using our previously developed mouse model [13]. Briefly, pregnant Imprinting Control Region (ICR) mice (age 8–12 weeks; CLEA Japan, Tokyo, Japan) were sacrificed and the blastocysts were retrieved from the uterine horns. The blastocysts were infected with adenoviral vectors encoding the human CD40L gene (Ad-CD40L; kindly provided by Dr. Fukushima, Eisai, Tokyo, Japan) and then transferred into the uterine horns of pseudopregnant ICR mice. (-)-Nicotine hydrogen tartrate salt (Sigma-Aldrich, St. Louis, MO) was administered to mice by osmotic pump (Alzet, Model 2002, Cupertino, CA) at a rate of 3 mg/kg/day. Maternal systolic blood pressure (BP) was measured each morning in triplicate by the tail-cuff method (BP-98E, Softron Co. Ltd., Tokyo, Japan) from embryonic day 8.5 (E8.5) through the day of delivery (E17.5). The mice were euthanized on E17.5 and live pups were weighed. All procedures were approved by the Animal Care and Use Committee of Ehime University.

##### 4.2. *Cell culture*

The human EVT cell line HTR-8/SVneo was provided by Dr. Charles H. Graham (Queen's University, Canada) and cultured at 37 °C and 5% CO<sub>2</sub> in phenol red-free Dulbecco's Modified Eagle Medium (DMEM, Thermo Fisher Scientific, Waltham, MA) supplemented with 10% fetal bovine serum (FBS), penicillin-streptomycin solution (Fujifilm Wako Pure Chemical Corp, Osaka, Japan), 1% L-glutamine (Thermo Fisher Scientific), 1 mM sodium pyruvate (Thermo Fisher Scientific), and 1% non-essential amino acids (Thermo Fisher Scientific).

##### 4.3. *Extraction of exosomes*

Subconfluent cultures were exchanged into DMEM with exosome-free FBS (Exo-FBS, System Biosciences, Palo Alto, CA) with or without 100  $\mu$ M nicotine and incubated for an additional 24 hr. Culture supernatants were collected and clarified by centrifugation at 3,000  $\times$  g for 15 min. The cleared supernatants were amended with ExoQuick-TC (System Biosciences) and incubated overnight at 4 °C to precipitate exosomes which were then collected by centrifugation at 1,500  $\times$  g for 30 min. The surface protein composition of the extracted exosomes was analyzed with an Exo-check exosome antibody array (Thermo Fisher Scientific) as shown in Supplementary Figure 1. After confirming the high purity and proper exosomal surface protein expression (CD81, CD63, and TSG101) of the preparation, the exosomes were resuspended in 50  $\mu$ L of Exosome Resuspension Buffer for proteomic analysis.

##### 4.4. *Proteomics sample preparation*

After cleanup of the sample with cold acetone (1:8 v/v, 2 h incubation at -20 °C), the protein fraction was sonicated in a lysis buffer (100 mM Tris, 0.5% sodium dodecanoic acid), quantitated using a BCA Assay Kit (Thermo Fisher Scientific), and adjusted to a total protein concentration of 1  $\mu$ g/ $\mu$ L in the lysis buffer. Following S-S bond cleavage and alkylation of cysteine residues, proteins were digested into peptides (with 400 ng Lys-C, 400 ng trypsin, 37 °C overnight), desalted on a C18 spin column, dried in a centrifugal

evaporator, and redissolved by sonication in sample buffer (3% acetonitrile with 0.1% formic acid, v/v) to a final peptide concentration of 200 ng/ $\mu$ L (as determined by BCA assay).

#### 4.5. Nano LC-MS analysis

Peptide samples were analyzed by nano LC-MS/MS (UltiMate 3000 RSLCnano LC System, Thermo Fisher Scientific) connected to a mass spectrometer (Q Exactive HF-X, Thermo Fisher Scientific). Samples were injected as 400 ng total peptide in 2  $\mu$ L of sample buffer, and the nano-LC column (2.7  $\mu$ m, 250  $\times$  0.075 mm, 100 Å) was run at a flow rate of 100 nL/min with the outflow monitored by an integrated emitter (CAPCELL CORE MP® C18, New Objective). An elution protocol of solvent A (0.1% formic acid, v/v), and solvent B (80% acetonitrile, 0.1% formic acid, v/v) was implemented with a gradual gradient from 1–39% solvent B over 82 min, followed by a steeper gradient of 39–80% solvent B over 14 min. As peptides eluted from the column and electrospray source, MS1 scans were acquired in the Orbitrap over the mass range 495–865 m/z at 120,000 resolution, followed by MS2 at 30,000 resolution.

#### 4.6. Statistical analysis

Physiologic data are represented as means  $\pm$  standard errors. We tested for statistical significance with the one-way analysis of variance using SPSS software (v27.0.0, IBM SPSS Statistics, Chicago, IL). Differences were considered significant at  $p < .05$ .

#### 4.7. DIA (Data Independent Acquisition) proteomic analysis

The LC-MS data were processed using Scaffold DIA (v2.1.0, Proteome Software Inc, Portland, OR), and we extracted only those proteins with an FDR  $< 1\%$ . We used a t-test to compare exosome protein content between the nicotine-treated and control groups. We considered  $p < .05$  to be statistically significant.

#### 4.8. Bioinformatic analysis

The proteins were annotated and classified using the Gene Ontology (GO) resource. Principal component analysis (PCA) was processed by Scaffold DIA. The interaction network of the proteins was analyzed by STRING (v11.0, String Consortium). Cytoscape (v3.8.0, Cytoscape Consortium) was used to identify hub proteins in the network by determining Degree Centrality and Between Centrality in the protein network.

## 5. Conclusions

Nicotine markedly alters the abundance of several proteins in EVT-derived exosomes, suggesting a mechanism by which tobacco smoke might influence the pathogenesis of PE. Further studies on these key proteins may provide insights into the mechanism of PE pathogenesis and the possibility of its prevention and treatment.

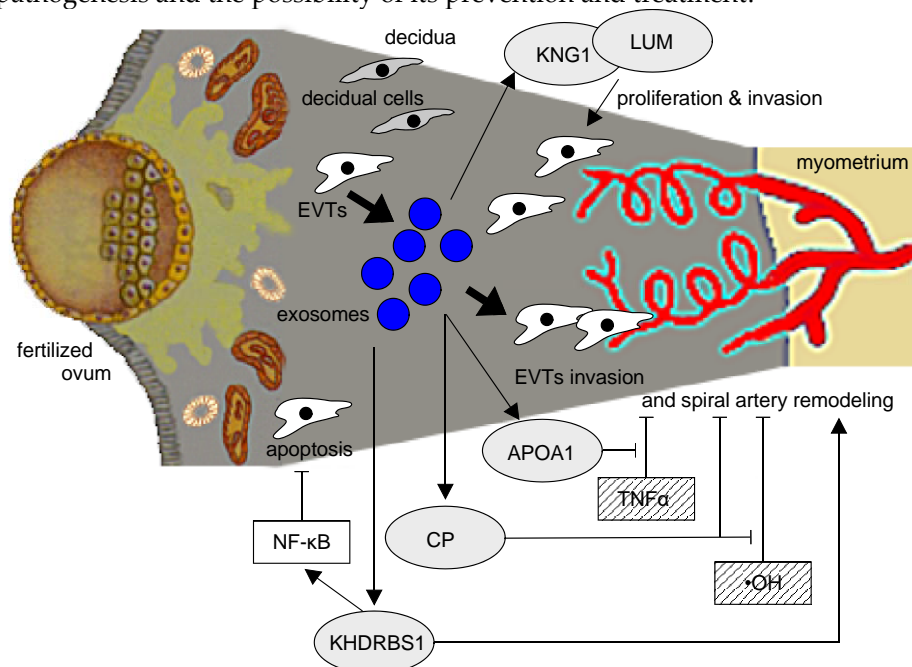


**Figure 8.** A model of the potential relationships between the five key proteins from our analysis and their influence on PE and EVTs. Kininogen, lumican, and KHDRBS1 are proteins more abundant in nicotine-treated EVT exosomes. These proteins promote cell proliferation and invasion, and KHDRBS1 further inhibits cell apoptosis via the activation of NF- $\kappa$ B signaling. APOA1 inhibits TNF $\alpha$ , and ceruloplasmin suppresses -OH and may rescue pathophysiology by improving cell proliferation and invasion of EVT in PE.

**Supplementary Materials:** The following supporting information can be downloaded at: [www.mdpi.com/xxx/s1](http://www.mdpi.com/xxx/s1), Figure S1: Antigen evaluation of exosomes using exosome-specific markers.

**Author Contributions:** Conceptualization, A.K. and K.M.; writing—original draft preparation, A.K. and K.M.; methodology, H.N.; formal analysis, A.K. and K.M.; data curation, A.K. and K.M.; review and editing, K.M.; supervision, Y.M. and T.S.; funding acquisition, K.M. All authors have read and agreed to the published version of the manuscript.

**Funding:** This work was funded by a Grant-in-Aid for Scientific Research from the Ministry of Education, Culture, Sports, Science and Technology of Japan (19K09781) and a grant from the Smoking Research Foundation (2018G024).

**Institutional Review Board Statement:** Not applicable.

**Informed Consent Statement:** Not applicable.

**Data Availability Statement:** Not applicable.

#### Conflicts of Interest

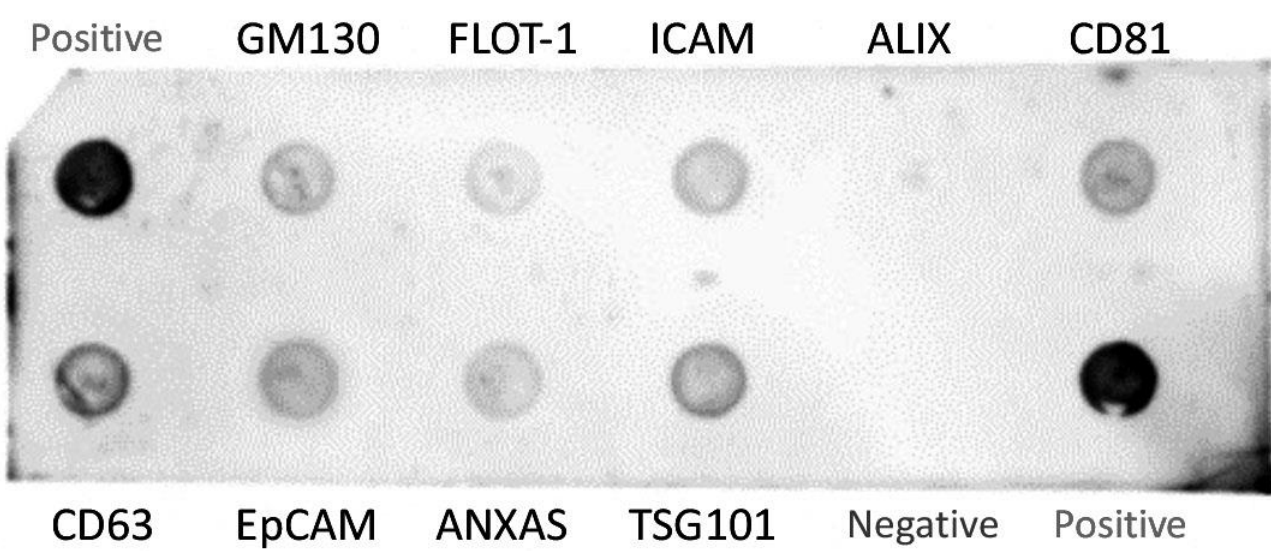
The authors declare no conflict of interest.

#### References

1. Granger, J.P.; Spradley, F.T.; Bakrania, B.A. The Endothelin System: A Critical Player in the Pathophysiology of Preeclampsia. *Curr. Hypertens. Rep.* **2018**, *20*, 32.
2. Kilbourn, R.G.; Traber, D.L.; Szabó, C. Nitric oxide and shock. *Dis. Mon.* **1997**, *43*, 277–348.
3. Matsubara, K.; Matsubara, Y.; Hyodo, S.; Katayama, T.; Ito, M. Role of nitric oxide and reactive oxygen species in the pathogenesis of preeclampsia. *J. Obstet. Gynaecol. Res.* **2010**, *36*, 239–247.
4. Walsh, S.W.; Wang, Y. Deficient glutathione peroxidase activity in preeclampsia is associated with increased placental production of thromboxane and lipid peroxides. *Am. J. Obstet. Gynecol.* **1993**, *169*, 1456–1461.
5. Redman, C.W.; Sargent, I.L. Placental stress and pre-eclampsia: a revised view. *Placenta*. **2009**, *30*, S38–42.
6. Roberts, J.M.; Hubel, C.A. The two stage model of preeclampsia: variations on the theme. *Placenta*. **2009**, *30*, S32–37.
7. Teng, X.; Chen, L.; Chen, W.; Yang, J.; Yang, Z.; Shen, Z. Mesenchymal Stem Cell-Derived Exosomes Improve the Microenvironment of Infarcted Myocardium Contributing to Angiogenesis and Anti-Inflammation. *Cell. Physiol. Biochem.* **2015**, *37*, 2415–2424.
8. England, L.; Zhang, J. Smoking and risk of preeclampsia: a systematic review. *Front. Biosci.* **2007**, *12*, 2471–2483.
9. Hammoud, A.O.; Bujold, E.; Sorokin, Y.; Schild, C.; Krapp, M.; Baumann, P. Smoking in pregnancy revisited: findings from a large population-based study. *Am. J. Obstet. Gynecol.* **2005**, *192*, 1856–1862.
10. West, R. Tobacco smoking: Health impact, prevalence, correlates and interventions. *Psychol. Health.* **2017**, *32*, 1018–1036.
11. Kaneko, S.; Maeda, T.; Kume, T.; Kochiyama, H.; Akaike, A.; Shimohama, S.; Kimura, J. Nicotine protects cultured cortical neurons against glutamate-induced cytotoxicity via  $\alpha 7$ -neuronal receptors and neuronal CNS receptors. *Brain. Res.* **1997**, *765*, 135–140.
12. Michalak, E.; Halko-Gasior, A.; Chomyszyn-Gajewska, M. The impact of tobacco on oral health - based on literature. *Przegl. Lek.* **2016**, *73*, 516–519.
13. Matsubara, K.; Matsubara, Y.; Mori, M.; Uchikura, Y.; Hamada, K.; Fujioka, T.; Hashimoto, H.; Matsumoto, T. Immune activation during the implantation phase causes preeclampsia-like symptoms via the CD40-CD40 ligand pathway in pregnant mice. *Hypertens. Res.* **2016**, *39*, 407–414.
14. Boswijk, E.; Bauwens, M.; Mottaghy, F.M.; Wildberger, J.E.; Bucerius, J. Potential of  $\alpha 7$  nicotinic acetylcholine receptor PET imaging in atherosclerosis. *Methods.* **2017**, *130*, 90–104.

15. Moccia, F.; Frost, C.; Berra-Romani, R.; Tanzi, F.; Adams, D.J. Expression and function of neuronal nicotinic ACh receptors in rat microvascular endothelial cells. *Am. J. Physiol. Heart. Circ. Physiol.* **2004**, *286*, H486–491.
16. Lee, W.O.; Wright, S.M. Production of endothelin by cultured human endothelial cells following exposure to nicotine or caffeine. *Metabolism*. **1999**, *48*, 845–848.
17. Mayhan, W.G.; Sharpe, G.M.; Anding, P. Agonist-induced release of nitric oxide during acute exposure to nicotine. *Life Sci.* **1999**, *65*, 1829–1837.
18. Nadler, J.L.; Velasco, J.S.; Horton, R. Cigarette smoking inhibits prostacyclin formation. *Lancet*. **1983**, *1*, 1248–1250.
19. Sharma, R.; Lodhi, S.; Sahota, P.; Thakkar, M.M. Nicotine administration in the wake-promoting basal forebrain attenuates sleep-promoting effects of alcohol. *J. Neurochem.* **2015**, *135*, 323–331.
20. Klisch, K.; Schraner, E.M. Intraluminal vesicles of binucleate trophoblast cell granules are a possible source of placental exosomes in ruminants. *Placenta*. **2020**, *90*, 58–61.
21. Su, Y.; Li, Q.; Zhang, Q.; Li, Z.; Yao, X.; Guo, Y.; Xiao, L.; Wang, X.; Ni, H. Exosomes derived from placental trophoblast cells regulate endometrial epithelial receptivity in dairy cows during pregnancy. *J. Reprod. Dev.* **2022**, *68*, 21–29.
22. Cooke, A.L.; Morris, J.; Melchior, J.T.; Street, S.E.; Jerome, W.G.; Huang, R.; Herr, A.B.; Smith, L.E.; Segrest, J.P.; Remaley, A.T.; et al. A thumbwheel mechanism for APOA1 activation of LCAT activity in HDL. *J. Lipid. Res.* **2018**, *59*, 1244–1255.
23. Charlton, F.; Bobek, G.; Stait-Gardner, T.; Price, W.S.; Mirabito Colafella, K.M.; Xu, B.; Makris, A.; Rye, K.A.; Hennessy, A. The protective effect of apolipoprotein in models of trophoblast invasion and preeclampsia. *Am. J. Physiol. Regul. Integr. Comp. Physiol.* **2017**, *312*, R40–48.
24. Fu, K.; Sun, X.; Wier, E.M.; Hodgson, A.; Liu, Y.; Sears, C.L.; Wan, F. Sam68/KHDRBS1 is critical for colon tumorigenesis by regulating genotoxic stress-induced NF- $\kappa$ B activation. *Elife*. **2016**, *5*, 10.
25. Erices, R.; Corthorn, J.; Lisboa, F.; Valdés, G. Bradykinin promotes migration and invasion of human immortalized trophoblasts. *Reprod. Biol. Endocrinol.* **2011**, *9*, 97.
26. Maurer, M.; Bader, M.; Bas, M.; Bossi, F.; Cicardi, M.; Cugno, M.; Howarth, P.; Kaplan, A.; Kojda, G.; Leeb-Lundberg, F.; et al. New topics in bradykinin research. *Allergy*. **2011**, *66*, 1397–1406.
27. Appunni, S.; Rubens, M.; Ramamoorthy, V.; Anand, V.; Khandelwal, M.; Saxena, A.; McGranaghan, P.; Odia, Y.; Kotecha, R.; Sharma, A. Lumican, pro-tumorigenic or anti-tumorigenic: A conundrum. *Clin. Chim. Acta*. **2021**, *514*, 1–7.
28. Giatagana, E.M.; Berdiaki, A.; Tsatsakis, A.; Tzanakakis, G.N.; Nikitovic, D. Lumican in Carcinogenesis-Revisited. *Biomolecules*. **2021**, *11*.
29. Chang, W.M.; Li, L.J.; Chiu, I.A.; Lai, T.C.; Chang, Y.C.; Tsai, H.F.; Yang, C.J.; Huang, M.S.; Su, C.Y.; Lai, T.L.; et al. The aberrant cancer metabolic gene carbohydrate sulfotransferase 11 promotes non-small cell lung cancer cell metastasis via dysregulation of ceruloplasmin and intracellular iron balance. *Transl. Oncol.* **2022**, *25*, 101508.
30. Yang, H.; Bao, Y.; Jin, F.; Jiang, C.; Wei, Z.; Liu, Z.; Xu, Y. Ceruloplasmin inhibits the proliferation, migration and invasion of nasopharyngeal carcinoma cells and is negatively regulated by miR-543. *Nucleotides. Nucleic. Acids*. **2022**, *41*, 474–488.
31. Chen, J.; Qiu, M.; Huang, Z.; Chen, J.; Zhou, C.; Han, F.; Qu, Y.; Wang, S.; Zhuang, J.; Li, X. Nicotine suppresses the invasiveness of human trophoblasts by downregulation of CXCL12 expression through the  $\alpha$ -7 subunit of the nicotinic acetylcholine receptor. *Reprod. Sci.* **2020**, *27*, 916–924.
32. Zong, Y.; Zhang, S.T.; Zhu, S.T. Nicotine enhances migration and invasion of human esophageal squamous carcinoma cells which is inhibited by nimesulide. *World. J. Gastroenterol.* **2009**, *15*, 2500–2505.
33. Zhang, J.; Klebanoff, M.A.; Levine, R.J.; Puri, M.; Moyer, P. The puzzling association between smoking and hypertension during pregnancy. *Am. J. Obstet. Gynecol.* **1999**, *181*, 1407–1413.
34. Han, X.; Li, W.; Li, P.; Zheng, Z.; Lin, B.; Zhou, B.; Guo, K.; He, P.; Yang, J. Stimulation of  $\alpha$ 7 nicotinic acetylcholine receptor by nicotine suppresses decidual M1 macrophage polarization against inflammation in lipopolysaccharide-induced preeclampsia-like mouse model. *Front. Immunol.* **2021**, *12*, 642071.
35. Liu, Y.; Yang, J.; Bao, J.; Li, X.; Ye, A.; Zhang, G.; Liu, H. Activation of the cholinergic anti-inflammatory pathway by nicotine ameliorates lipopolysaccharide-induced preeclampsia-like symptoms in pregnant rats. *Placenta*. **2017**, *49*, 23–32.
36. Morisaki, N.; Obara, T.; Piedvache, A.; Kobayashi, S.; Miyashita, C.; Nishimura, T.; Ishikuro, M.; Sata, F.; Horikawa, R.; Mori, C.; et al. Association between smoking and hypertension in pregnancy among Japanese women: a meta-analysis of birth cohort studies in the Japan Birth Cohort Consortium (JBiCC) and JECS. *J. Epidemiol.* **2022**, *10*, 2188.
37. Kawashima, A.; Koide, K.; Hasegawa, J.; Arakaki, T.; Takenaka, S.; Maruyama, D.; Matsuoka, R.; Sekizawa, A. Maternal smoking history enhances the expression of placental growth factor in invasive trophoblasts at early gestation despite cessation of smoking. *PLoS. One*. **2015**, *10*, e0134181.
38. Pillay, P.; Moodley, K.; Moodley, J.; Mackraj, I. Placenta-derived exosomes: potential biomarkers of preeclampsia. *Int. J. Nano-medicine*. **2017**, *12*, 8009–8023.
39. Matsubara, K.; Abe, E.; Ochi, H.; Kusanagi, Y.; Ito, M. Changes in serum concentrations of tumor necrosis factor alpha and adhesion molecules in normal pregnant women and those with pregnancy-induced hypertension. *J. Obstet. Gynaecol. Res.* **2003**, *29*, 422–426.





**Supplementary Figure 1.** Antigen evaluation of exosomes using exosome-specific markers